

Ion Transport across Planar Bilayer Lipid Membrane Driven by D-Fructose Dehydrogenase-catalyzed Electron Transport

Keisuke Sasakura, Osamu Shirai,* Kei Hichiri, Maiko Goda-Tsutsumi, Seiya Tsujimura, and Kenji Kano
Division of Applied Life Sciences, Graduate School of Agriculture, Kyoto University, Sakyo-ku, Kyoto 606-8502

(Received February 17, 2011; CL-110133; E-mail: shiraio@kais.kyoto-u.ac.jp)

Electron transport catalyzed by a membrane-bound enzyme, D-fructose dehydrogenase (FDH), from one aqueous phase (W1) containing D-fructose to another one (W2) containing $[\text{Fe}(\text{CN})_6]^{3-}$ across a planar bilayer lipid membrane (BLM) containing 7,7,8,8-tetracyanoquinodimethane (TCNQ) was investigated electrochemically. We found that the ion transport across the BLM was driven at the same time by the electromotive force generated by the electron transport.

Enzyme-catalyzed reactions play important roles in respiration, metabolism, etc. Several studies have been made on enzyme-catalyzed electron transport in biomembranes.^{1–3} The electron-transport mechanisms, however, are not well understood owing mainly to the complexity of living organisms. On the other hand, some voltammetric studies have been reported to examine the electron transport across self-assembled monolayer (SAM) films and bilayer lipid membranes (BLMs), which are coated on the surface of solid electrodes, in the presence of redox compounds and redox proteins.^{4–6} The electron transport, which is catalyzed by a membrane-bound enzyme, between two aqueous phases across BLM like a biomembrane, however, has never been studied.

Fructose dehydrogenase (FDH) from *Gluconobacter frateurii* is a membrane-bound enzyme with a molecular mass of ca. 140 kDa containing FAD and three hemes *c* as the prosthetic groups.^{7–9} FDH works as a catalyst of two-electron oxidation of D-fructose to 5-keto-D-fructose.¹⁰ However, the details on the electron transport across BLM between two aqueous phases remain to be elucidated. In addition, not only the electron transport but the ion transport should be considered in this case, because ionic species should locate to maintain electroneutrality in all phases.

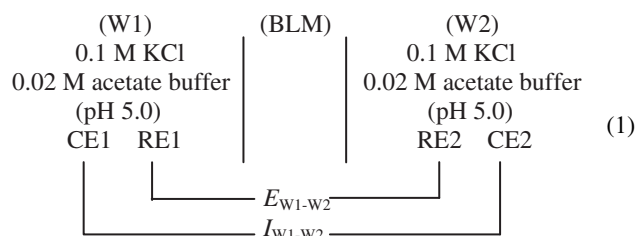
In this study, FDH-catalyzed electron transport across a planar BLM was examined by cyclic voltammetry in the presence of 7,7,8,8-tetracyanoquinodimethane (TCNQ) in the BLM as an electron-transport mediator. The coupling reaction between the transport of ions existing in aqueous phases across the BLM and the FDH-catalyzed electron transport is investigated in order to elucidate the mechanism of the ion transport driven by the electron transport across cell membranes in living organisms. Lecithin (PC, Wako Pure Chemical Ind., Ltd.) and cholesterol (Ch, Kanto Chemical Co., Inc.) were used to form BLM. BLM-forming solution was prepared by dissolving a mixture of about 10 mg of PC and about 5 mg of Ch in 1 mL of *n*-decane. TCNQ (Adrich Chemical Co., Inc.) was used as a redox compound in BLM. In order to prepare TCNQ-containing BLM, another BLM-forming solution was prepared by dissolving 10 mg of PC and 5 mg of Ch in 1 mL of a 1:9 mixture of 1,2-dichloroethane (DCE) containing TCNQ and *n*-decane. The concentration of TCNQ in the DCE solution was adjusted to

10 mM, and it was confirmed by UV–vis spectrophotometry (Shimadzu Co., UV-2550) that a small portion of TCNQ in the BLM-forming solution was reduced to one-electron-reduced form ($\text{TCNQ}^{\cdot-}$).¹¹

D-Fructose dehydrogenase (FDH) from *Gluconobacter* sp. was purchased from Toyobo Enzymes Co. and used without further purification. All other reagents were of reagent grade.

The electrochemical cell used for voltammetric measurements with the BLM system was the same as that used in previous work.^{12,13} The BLM was constructed as a black lipid membrane by brushing the BLM-forming solution on a 0.8 mm diameter aperture created on a tetrafluoroethylene resin sheet of the electrochemical cell. The formation of the BLM was confirmed by microscopic observations and capacitance measurements.¹²

The electrochemical cell employed in the present study is indicated by eq 1.



The cell has two aqueous compartments separated by a 0.2 mm thick tetrafluoroethylene resin sheet, and the two compartments were filled with 15 mL of aqueous solution. It was then placed in a Faraday cage in order to decrease the background noise during electrochemical measurements. Voltammetric measurements were performed on a four-electrode potentiostat (Hokuto Denko Co., HA1010mM1A), a function generator (Hokuto Denko Co., HB-105), and an A/D converter (Graphtec Co., GL500A). The potential difference, $E_{\text{W1-W2}}$, was applied between two Ag|AgCl electrodes (RE1 and RE2) and the current, $I_{\text{W1-W2}}$, between two Pt wire electrodes (CE1 and CE2) was recorded. The current density, $j_{\text{W1-W2}}$, was evaluated by dividing $I_{\text{W1-W2}}$ by the BLM area. All voltammograms were measured at a scan rate of 10 mV s^{-1} and at $25 \pm 1^\circ\text{C}$, unless otherwise mentioned. Curve 1 in Figure 1 shows a cyclic voltammogram between W1 and W2 of 0.02 M acetate buffer containing 0.1 M KCl across the BLM in the absence of TCNQ. In this case, Faradaic current due to the transfer of neither ion nor electron was observed in the voltammogram, indicating that the BLM serves as a barrier to the permeation of hydrophilic ions such as K^+ or Cl^- . In the presence of TCNQ in the BLM between two 0.02 M aqueous potassium acetate buffer (pH 5.0) solutions containing 0.1 M KCl, a symmetric sigmoidal curve about the origin (0 V, 0 A) was observed, as shown by curve 2 in Figure 1. The anodic and the cathodic currents flowed between

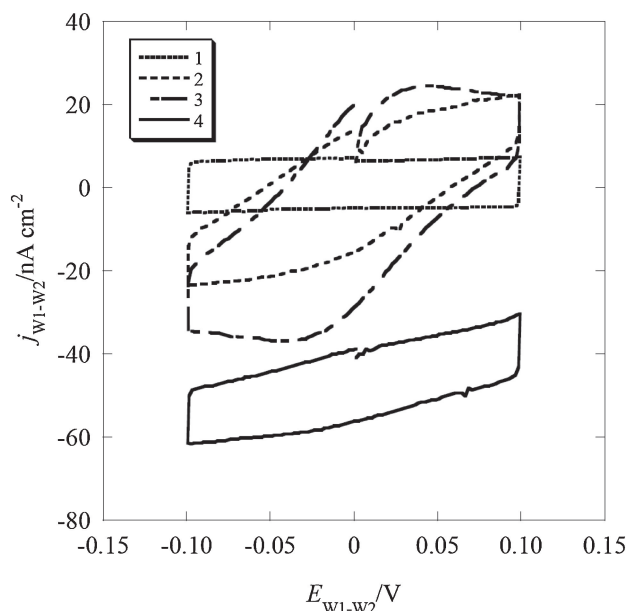


Figure 1. Cyclic voltammograms for charge transfer across the BLM containing 1 mM TCNQ. Curve 1: 0.1 M KCl and 0.02 M potassium acetate buffer (pH 5.0) in W1 and W2. Curve 2: as curve 1, but in the presence of 1 mM TCNQ in the BLM forming solution. Curve 3: as curve 2, but in the presence of 0.05 M D-fructose and 2×10^{-8} M FDH in W1. Curve 4: as curve 3, but in the presence of 1 mM $K_3[Fe(CN)_6]$ in W2.

W1 and W2 across the BLM. Here, it is defined that the positive current is caused by the transport of K^+ from W1 to W2 and/or that of $TCNQ^{\bullet-}$ or electron from W2 to W1. Conversely, the negative current is caused by the transport of K^+ from W2 to W1 and/or by that of $TCNQ^{\bullet-}$ or electron from W1 to W2. When TCNQ, including $TCNQ^{\bullet-}$, was added into the BLM, it is thought that a small part of K^+ was dissolved from the aqueous phases to the BLM with $TCNQ^{\bullet-}$ as a counter ion. Then, $TCNQ^{\bullet-}$ may in part transport between W1 and W2 across the BLM, and it also serves as a carrier of K^+ in the BLM, respectively.¹² It has been reported that K^+ is distributed as the counter ion of $TCNQ^{\bullet-}$ and that the transport of K^+ between W1 and W2 across a BLM occurs mainly in a similar cell system.¹⁴ Therefore, the current observed was mainly attributed to the transport of K^+ , as shown in Figure 2a.

In the presence of 2×10^{-8} M FDH and 0.05 M D-fructose in W1, curve 3 of Figure 1 was obtained. FDH was added as an aqueous solution dissolved by detergent. As for D-fructose, 2 M D-fructose was prepared as a stock solution, and the solution was added into W1 in order to be adjusted to 0.05 M. When either of FDH and D-fructose was added into W1, the cyclic voltammogram remained unchanged and was the same as curve 2 in Figure 1. The adsorption of FDH at the surface of the lipid layer was confirmed by quartz crystal microbalance using the solid-supported BLM. On the other hand, the cyclic voltammogram was the same as curve 1 in Figure 1 in the absence of TCNQ and $TCNQ^{\bullet-}$ in the BLM even in the presence of both FDH and D-fructose in W1. FDH catalyzes two-electron oxidation of D-fructose as written by eq 2¹⁰ and then donates the electron to TCNQ in the BLM at the W1|BLM interface as eq 3.

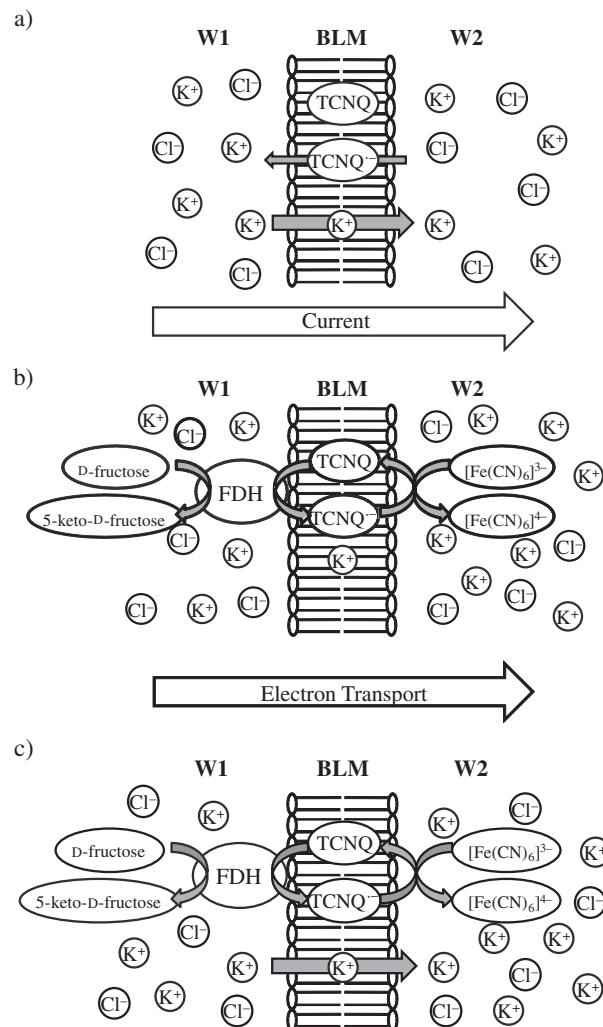


Figure 2. Schematic models of charge transports. (a) The ion transport across the BLM in the presence of $TCNQ^{\bullet-}$. (b) The FDH-catalyzed electron transport across the BLM in the presence of TCNQ and $TCNQ^{\bullet-}$. (c) The ion-transport coupling with the electron transport.



Here, subscripts (Ox and Red) signify oxidized and reduced forms of FDH immobilized on the BLM surface.

As a result, the concentration of $TCNQ^{\bullet-}$ in the BLM was increased by the electron-transport reaction from FDH_{Red} to $TCNQ$ at the W1|BLM interface. In order to maintain the electroneutrality in the BLM, the concentration of K^+ in the BLM should increase with an increase of the $TCNQ^{\bullet-}$ concentration in the BLM. The increase in the concentrations of K^+ and $TCNQ^{\bullet-}$ in the BLM is predominantly responsible for the increase in current of the cathodic and anodic waves. In addition, the waveform of curve 3 in Figure 1 as a whole seems to be shifted in the negative direction. Since small amounts of $TCNQ^{\bullet-}$ and $TCNQ$ were spontaneously distributed from the BLM to W1 and W2, $TCNQ$ in W1 and W2 seems to be reduced by $TCNQ^{\bullet-}$, which was supplied to the BLM by the reaction

between FDH_{Red} and TCNQ at the W1|BLM interface, in the BLM. The negative shift of the waveform is quite likely attributed to the electron transport caused by coupling of the reduction of TCNQ in the BLM to $\text{TCNQ}^{\bullet-}$ by FDH_{Red} with the reduction of TCNQ in W2 to $\text{TCNQ}^{\bullet-}$ by $\text{TCNQ}^{\bullet-}$ in the BLM.

In the presence of 2×10^{-8} M FDH and 0.05 M D-fructose in W1, of $\text{TCNQ}^{\bullet-}$ in the BLM and of 0.001 M $\text{K}_3[\text{Fe}(\text{CN})_6]$ in the W2 phase, curve 4 was obtained as shown in Figure 1. The negative current was observed in the potential range between -0.10 and 0.10 V. The negative current was caused by coupling the electron transport from the W1 phase to the BLM due to the reduction of TCNQ by FDH_{Red} at the W1|BLM interface to that from the BLM to the W2 phase due to the reduction of $[\text{Fe}(\text{CN})_6]^{3-}$ in the W2 phase by $\text{TCNQ}^{\bullet-}$ in the BLM. TCNQ thus served as carrier in the BLM. Then, the catalytic oxidation of D-fructose by FDH_{Ox} at the W1|BLM interface seems to be promoted by the electron transport across the BLM between W1 and W2. On the other hand, the negative current was also observed, when flavin adenine dinucleotide dependent glucose dehydrogenase (FAD-GDH), which is a soluble enzyme in aqueous phase, and D-glucose were added into the W1 phase instead of FDH and D-fructose. The magnitude of the negative current in the case of FAD-GDH, however, was much smaller than that in the present case. This indicates that the membrane-bound enzyme works more efficiently than the water-soluble enzyme. Figure 2b shows the scheme on the electron transport between W1 and W2 across the BLM in the present system. Incidentally, the total charge transport between W1 and W2 across the BLM is caused by the coupling of the electron transport with the ion transport of K^+ and $\text{TCNQ}^{\bullet-}$. In the present case, TCNQ molecules play important roles not only in the electron transport but in the ion transport. The slope around 0 V of curve 4 was much smaller than that of curve 3. This seems to be ascribed to the situation that the major part of $\text{TCNQ}^{\bullet-}$ in the BLM serves as an electron-transport mediator and that the concentration profile of $\text{TCNQ}^{\bullet-}$ reaches a steady state. The electromotive force is generated by the electron transport in this case, and it drives the transport of K^+ from W1 to W2 across the BLM. At the zero-current membrane potential, the number of electrons transported from W1 to W2 is almost equal to that of K^+ transported from W1 to W2. Since the electric current does not flow totally across cell membranes in living cells to maintain electroneutrality, it seems reasonable to assume that the ion transport is in proportion to the electron transport at the zero-current membrane potential. The zero-current membrane potential could not be measured unfortunately in the present experiment, because the BLM was fragile at potential more positive than 0.1 V. But it is obvious from curve 4 in Figure 1 that the zero-current membrane potential is present at potential more positive than 0.1 V. In the present work,

the transport of K^+ from W1 to W2 and the transport of $\text{TCNQ}^{\bullet-}$ from W2 to W1 are facilitated by the electron transport, as shown in Figure 2c. It is not too much to say that the coupling reaction is one of ion pump systems. In addition, the coupling between the electron transport and the ion transport seems to depend on the charge transport at the W1|BLM and BLM|W2 interfaces based on the knowledge of charge-transfer voltammetry at the interface between two immiscible electrolyte solutions.^{15,16} The electron transport across the BLM is always coupled with the ion transport of coexisting ions in order to maintain the electroneutrality in W1, BLM, and W2. When the electromotive force is produced by the electron transport, the ion transport is driven by the electron transport. The coupling mechanism seems to be useful to interpret the function of ion pumps and the energy conversion system.

This work was supported in part by a Grant-in-Aid for Scientific Research from the Ministry of Education, Culture, Sports, Science and Technology of Japan (to O.S.).

References

- 1 E. Kennett, P. Kuchel, *IUBMB Life* **2003**, *55*, 375.
- 2 P. R. Rich, *Biochim. Biophys. Acta, Rev. Bioenerg.* **1984**, *768*, 53.
- 3 B. L. Trumppower, *J. Bioenerg. Biomembr.* **1981**, *13*, 1.
- 4 E. Sackmann, *Science* **1996**, *271*, 43.
- 5 L. J. C. Jeuken, S. D. Connell, P. J. F. Henderson, R. B. Gennis, S. D. Evans, R. J. Bushby, *J. Am. Chem. Soc.* **2006**, *128*, 1711.
- 6 H. T. Tien, S. H. Wurster, A. L. Ottova, *Bioelectrochem. Bioenerg.* **1997**, *42*, 77.
- 7 M. Ameyama, O. Adachi, *Methods Enzymol.* **1982**, *89*, 154.
- 8 Y. Kamitaka, S. Tsujimura, N. Setoyama, T. Kajino, K. Kano, *Phys. Chem. Chem. Phys.* **2007**, *9*, 1793.
- 9 M. Tominaga, S. Nomura, I. Taniguchi, *Biosens. Bioelectron.* **2009**, *24*, 1184.
- 10 Y. Yamada, K. Aida, T. Uemura, *Agric. Biol. Chem.* **1966**, *30*, 95.
- 11 L. R. Melby, R. J. Harder, W. R. Hertler, W. Mahler, R. E. Benson, W. E. Mochel, *J. Am. Chem. Soc.* **1962**, *84*, 3374.
- 12 O. Shirai, Y. Yoshida, M. Matsui, K. Maeda, S. Kihara, *Bull. Chem. Soc. Jpn.* **1996**, *69*, 3151.
- 13 P. Krysinski, H. T. Tien, *Bioelectrochem. Bioenerg.* **1988**, *19*, 227.
- 14 H. Shiba, K. Maeda, N. Ichieda, M. Kasuno, Y. Yoshida, O. Shirai, S. Kihara, *J. Electroanal. Chem.* **2003**, *556*, 1.
- 15 J. Hanzlik, Z. Samec, J. Hovorka, *J. Electroanal. Chem. Interfacial Electrochem.* **1987**, *216*, 303.
- 16 H. Hotta, N. Akagi, T. Sugihara, S. Ichikawa, T. Osakai, *Electrochem. Commun.* **2002**, *4*, 472.